Extraction of Tantalum and Niobium from Tin Slags by Chlorination and Carbochlorination

I. GABALLAH, E. ALLAIN, and M. DJONA

Chlorination and carbochlorination of tantalum and niobium low-grade concentrate (LGC) and high-grade concentrate (HGC), obtained by leaching of tin slag, were studied using $Cl_2 + N_2$ and $Cl_2 + CO + N_2$ gas mixtures. Thermogravimetric analysis and conventional boat experiments were performed between 200 °C and 1000 °C. Chemical analysis, X-ray diffraction (XRD), and scanning electron microscopy (SEM) were used to characterize the samples and reaction products. Chlorination of LGC led to the recovery of about 95 pct of tantalum and niobium compounds at 1000 °C. However, the tantalum and niobium chlorinated compounds were contaminated by chlorides of Fe, Mn, *etc.* For HGC, chlorination at 1000 °C allowed the extraction of about 84 and 65 pct of the niobium and tantalum compounds, respectively. The recovered condensates were composed of pure tantalum and niobium chlorinated compounds. The apparent activation energies E_a for the chlorination of LGC and HGC, between 850 °C and 1000 °C, were 166 and 293 kJ/mole, respectively. At temperatures lower than 650 °C, the apparent activation energies for the LGC and HGC carbochlorination were 116 and 103 kJ/mole, respectively. Total extraction of the tantalum and niobium compounds was achieved by the carbochlorination of the LGC at 1000 °C. The generated tantalum and niobium chlorinated compounds were contaminated by the chlorides of Fe, Mn, Al, and Ca. The carbochlorination of the HGC at 500 °C allowed complete extraction and recovery of pure tantalum and niobium compounds. These results confirm the importance of obtaining an HGC from tin slag before its subsequent chlorination. The carbochlorination of such a concentrate could be an efficient process for the recovery of relatively pure tantalum and niobium chlorinated compounds at low temperatures.

I. INTRODUCTION

NIOBIUM and tantalum are important elements used in many high-technology applications such as electronic, energy, superconductors, and aerospace.[1,2] Industrialized countries consume the majority of the world production (≥95 pct) of these refractory metals and produce less than 5 pct.[3]

These elements are not abundant in the earth's crust. The average content of Nb and Ta in the earth's crust (Clarke*)[4] are 20 and 2.3 ppm, respectively. This may explain the high price of their concentrate (about 30 US$/lb.[5]) Their main bearing minerals are pyrochlore, microlite, tantalite, columbite, and columbo-tantalite. These minerals are often associated to cassiterite. The mineral processing of these ores leads to a cassiterite (SnO_2) concentrate containing up to 2 pct of Nb and Ta oxides as mixed grains or inclusions.[6] During the pyrometallurgical extraction of tin from cassiterite, oxides of Ta, Nb, Ti, Zr, rare earth elements, Si, Fe, Al, and Ca are concentrated in the slag.

*Average content of a specific element in the earth's crust.

Conventional methods used for the extraction of niobium and tantalum compounds from tin slags consist of full dissolution with HF, $HF + H_2SO_4$,[7] or smelting in electric furnaces.[8] Currently, these processes are limited either by economic or by environmental considerations.[9]

Due to the currently low metal market and new environmental regulations, more efficient, flexible and environmentally friendly processes are required for the extraction of these metals from ores, industrial byproducts, or wastes. The recovery of tantalum and niobium from tin slag was carried out in our laboratory using a two-step process of leaching[10] followed by the chlorination or the carbochlorination of the resulting concentrates.

This article focuses on the kinetics of chlorination and carbochlorination of these tantalum- and niobium-bearing concentrates with Cl_2-N_2 and Cl_2-CO-N_2 gas mixtures. Two concentrates differentiated by their tantalum and niobium oxide contents were used in this study. They were designated as low-grade concentrate (LGC) and high-grade concentrate (HGC).

II. LITERATURE REVIEW

Almost all the publications related to the chlorination of tin slag for the extraction of tantalum and niobium compounds focused on the use of chlorine and carbon.[11–16] The literature review indicated that direct chlorination of tin slag without pretreatment is an inefficient process. This was due to the formation of solid and/or liquid ferrous, calcium,

I. GABALLAH, Senior Researcher, Laboratoire Environnement et Minéralurgie, associated with the Centre National de la Recherche Scientifique, Mineral Processing and Environmental Engineering Team, INPL-ENSG, rue du Doyen M. Roubault, BP 40, 54501 Vandoeuvre Cedex, France. E. ALLAIN, formerly Research Associate with the Mineral Processing and Environmental Engineering Team, is Postdoctoral Research Associate with INASMET, Camino de Portuexte 12, 20009 San Sebastian, Spain. M. DJONA, formerly Research Associate with the Mineral Processing and Environmental Engineering Team, is Postdoctoral Research Associate with the Université du Québec, Institut National de la Recherche Scientifique, INRS-Géoressources, Complexe Scientique, 2700 rue Einstein, CP 7500, Sainte Foy, G1V 4C7 Canada.

Manuscript submitted October 31, 1994.

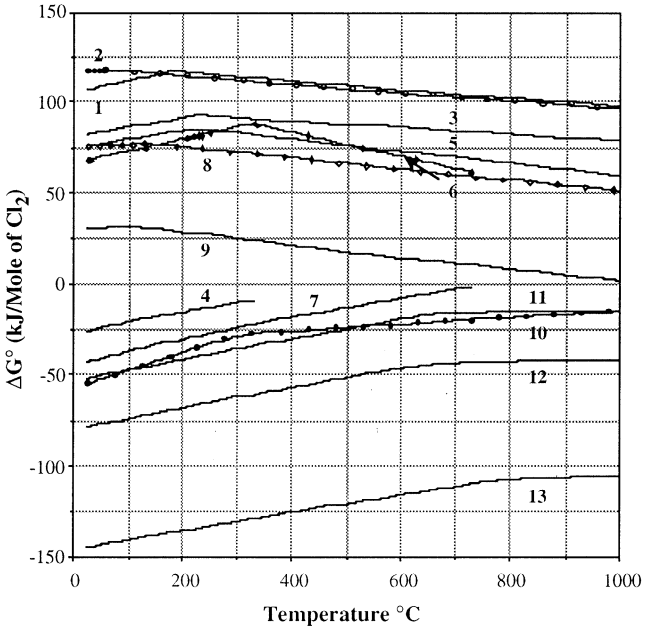

1/3	Al_2O_3	+	Cl_2	→	2/3	$AlCl_3$	+	1/2 O_2	[1]
1/2	SiO_2	+	Cl_2	→	1/2	$SiCl_4$	+	1/2 O_2	[2]
1/5	Ta_2O_5	+	Cl_2	→	2/5	$TaCl_5$	+	1/2 O_2	[3]
	Ta_2O_5	+	Cl_2	→	2	TaO_2Cl	+	1/2 O_2	[4]
1/5	Nb_2O_5	+	Cl_2	→	2/5	$NbCl_5$	+	1/2 O_2	[5]
1/3	Nb_2O_5	+	Cl_2	→	2/3	$NbOCl_3$	+	1/2 O_2	[6]
	Nb_2O_5	+	Cl_2	→	2	NbO_2Cl	+	1/2 O_2	[7]
1/2	TiO_2	+	Cl_2	→	1/2	$TiCl_4$	+	1/2 O_2	[8]
1/2	SnO_2	+	Cl_2	→	1/2	$SnCl_4$	+	1/2 O_2	[9]
2/3	FeO	+	Cl_2	→	1/3	$FeCl_3$	+	1/3 O_2	[10]
	FeO	+	Cl_2	→		$FeCl_2$	+	1/2 O_2	[11]
	MnO	+	Cl_2	→		$MnCl_2$	+	1/2 O_2	[12]
	CaO	+	Cl_2	→		$CaCl_2$	+	1/2 O_2	[13]

Fig. 1—Standard free energy changes of chlorination of oxides contained in the concentrates, as calculated by HSC.[19]

manganese, and other chlorides or to the contamination of the tantalum and niobium chlorinated compounds by impurities such as ferric chloride.[11,12,14,15,16] To overcome this inconvenience, partial removal of the above mentioned impurities was reported by several investigators[13,15,16,17] using chemical leaching of tin slag. The subsequent chlorination of the residue produced a mixture of niobium and tantalum oxychlorides and/or chlorides containing fewer impurities.

In previous investigations,[10,18] it was possible to obtain a concentrate containing about 78 pct of tantalum and niobium oxides almost free of Fe, Ca, Al, and Mn impurities. Chlorination of such HGCs is expected to reduce reagent costs and energy consumption. In addition, the extracted tantalum and niobium chlorinated compounds will have higher purity compared to those obtained by the chlorination of LGCs.

III. THERMODYNAMICS

Figure 1 gives the standard free energy changes of chlorination of some oxides contained in the tin slag concentrates. All the thermodynamic data were calculated using the HSC thermochemical database software.[19] At 500 °C, oxides could be classified as a function of the decreasing thermodynamic probabilities of their chlorination, as follows:

$$\underline{CaO} > \underline{MnO} > \underline{FeO} > \underline{Nb_2O_5} > \underline{Ta_2O_5} > \underline{SnO_2} > TiO_2 > SiO_2 \approx Al_2O_3$$

From the thermodynamic point of view, the chlorination of the underlined oxides by chlorine, at temperatures lower than 1000 °C, is much more favorable than the other oxides.

The standard free energy changes of carbochlorination of same oxides are given in Figure 2 as a function of temperature between 25 °C and 1000 °C. As expected, the carbochlorination reactions with the Cl_2 + CO gas mixture are thermodynamically more favorable than those of the chlorination with Cl_2. At temperatures lower than 1000 °C, it is expected that all the oxides will be carbochlorinated in decreasing order as follows:

$$CaO > MnO > FeO > SnO_2 > TiO_2 > Nb_2O_5 > Ta_2O_5 > SiO_2 \approx Al_2O_3$$

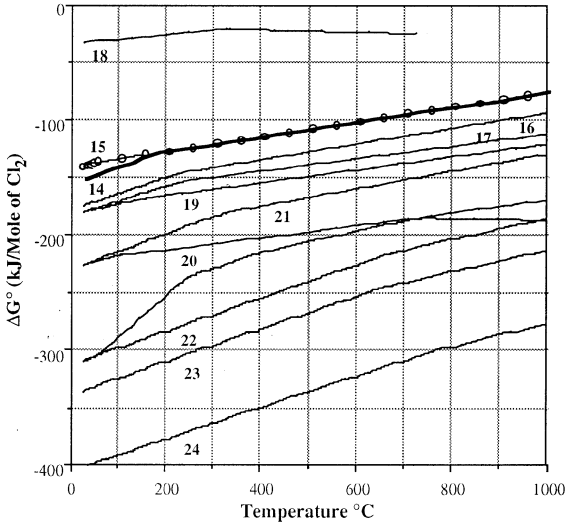

1/3	Al_2O_3	+	Cl_2	+	CO	→	2/3	$AlCl_3$	+	CO_2 [14]
1/2	SiO_2	+	Cl_2	+	CO	→	1/2	$SiCl_4$	+	CO_2 [15]
1/5	Ta_2O_5	+	Cl_2	+	CO	→	2/5	$TaCl_5$	+	CO_2 [16]
1/5	Nb_2O_5	+	Cl_2	+	CO	→	2/5	$NbCl_5$	+	CO_2 [17]
1/3	Nb_2O_5	+	Cl_2	+	CO	→	2/3	$NbOCl_3$	+	CO_2 [18]
1/2	TiO_2	+	Cl_2	+	CO	→	1/2	$TiCl_4$	+	CO_2 [19]
1/2	SnO_2	+	Cl_2	+	CO	→	1/2	$SnCl_4$	+	CO_2 [20]
2/3	FeO	+	Cl_2	+	2/3 CO	→	1/3	$FeCl_3$	+	2/3 CO_2 [21]
	FeO	+	Cl_2	+	CO	→		$FeCl_2$	+	CO_2 [22]
	MnO	+	Cl_2	+	CO	→		$MnCl_2$	+	CO_2 [23]
	CaO	+	Cl_2	+	CO	→		$CaCl_2$	+	CO_2 [24]

Fig. 2—Standard free energy changes of carbochlorination of oxides contained in the concentrates, as calculated by HSC.[19]

IV. EXPERIMENTAL

A. *Materials*

The average composition of the tin slag and the two concentrates is given in Table I. The LGC was obtained by a conventional acid (HCl) leaching of the slag. Besides tantalum and niobium oxides, this sample contains important amounts of Si, Al, Ca, Fe, Mn, and traces of other oxides. The HGC was obtained as the final residue of a successive acid and basic (HCl followed by NaOH) leaching of the tin slag.[10,18,20] In this case, the majority of Fe, Ca, Mn, Al,

Table I. Chemical Composition of the Tin Slag and Leaching Concentrates (Weight Percent)

Sample	Nb_2O_5	Ta_2O_5	SiO_2	CaO	FeO	Al_2O_3	SnO_2	MnO	K_2O	TiO_2	H_2O
Slag	5.2	7.5	41.9	11.6	3.3	11.2	0.7	3.7	1.4	1.3	≈0
LGC*	6.3	13.7	43.3	9.8	2.5	5.2	0.9	2.3	0.8	1.2	≈5
HGC**	28.0	31.1	10.0	0.6	0.2	0.6	0.2	0.0	0.4	1.4	≈20

*Low-grade concentrate.
**High-grade concentrate.

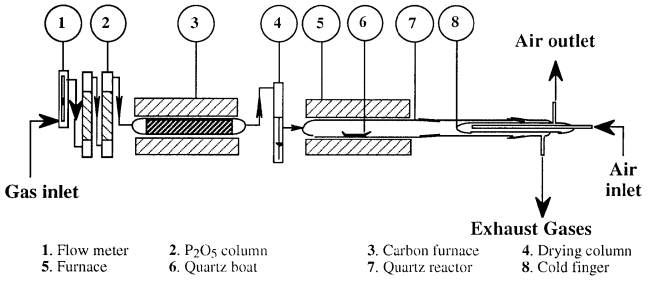

Fig. 3—Horizontal apparatus for the chlorination and carbochlorination tests.

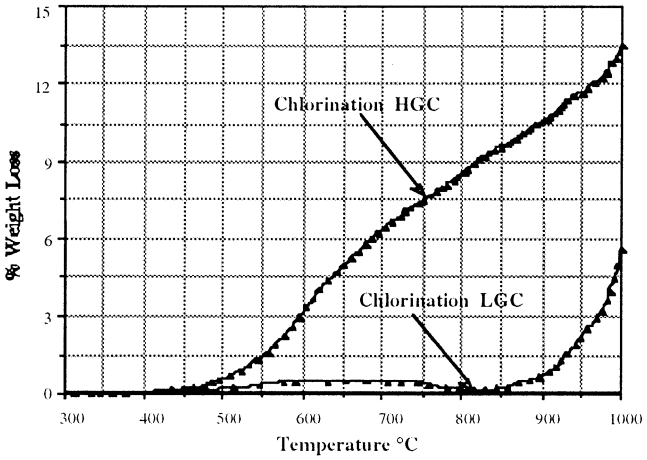

Fig. 4—Chlorination of LGC and HGC, under nonisothermal conditions (heating rate = 25 °C/min) using a chlorinating gas mixture having a Cl_2/N_2 ratio equal to one and a flow rate of 20 L/h.

etc., oxides were eliminated. This will facilitate the subsequent chlorination of HGC and may lead to pure tantalum and niobium compounds. The resulting HGC concentrate contains about 60 pct $Ta_2O_5 + Nb_2O_5$. Several lots of HGC, obtained by leaching different samples of tin slag, were used in this study as represented by the average composition in Table I.

B. *Apparatus and Experimental Procedure*

The kinetic study was carried out using the thermogravimetric analysis (TGA) apparatus detailed in Reference 21. The experimental procedure was similar to that described in this reference. The characterization of the reaction products by X-ray diffraction (XRD), scanning electron microscopy (SEM), chemical analysis, *etc.*, needs larger quantities of material than those produced during the TGA trials. For this reason, 5 g of the leaching concentrates were chlorinated between 200 °C and 1000 °C, over a period of 24 hours using the experimental apparatus shown schematically in Figure 3. Volatile oxychlorides and/or chlorides

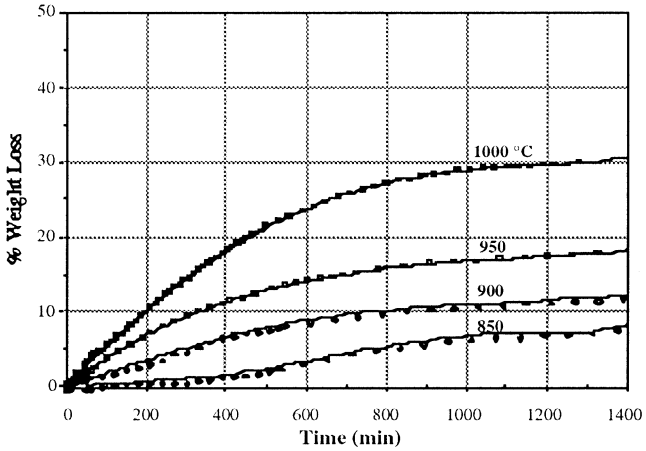

Fig. 5—Isotherms of the LGC chlorination using a chlorinating gas mixture having a Cl_2/N_2 ratio equal to one and a flow rate of 20 L/h.

were recovered in a cold finger maintained at room temperature by air circulation. Residues and condensates were subjected to chemical analysis and XRD. The residues analyzed by SEM were preliminarily decomposed by heating in a nitrogen atmosphere to avoid the formation of hydrated metal chlorides that are hygroscopic.

V. RESULTS AND DISCUSSION

A. *Chlorination of the Low- and High-Grade Concentrates by $Cl_2 + N_2$*

1. *Kinetic study*

The kinetics of chlorination of LGC and HGC was studied using nonisothermal thermogravimetric (TG) measurements. In both cases, a $Cl_2 + N_2$ (1/1) gas mixture with a total flow rate of 20 L/h (average velocity ≈ 0.22 cm/s) was used. The furnace heating rate was 25 °C/min. Figure 4 compares the chlorination weight loss of the LGC to that of the HGC as a function of temperature. It should be noted that the chlorination of the HGC and LGC started at about 400 °C. However, at a given temperature, the weight loss of the HGC was higher than that of the LGC.

The evolution of the chlorination weight loss of the LGC and HGC as a function of time at different temperatures is given in Figures 5 and 6, respectively. These figures indicate that the chlorination of both samples was incomplete even at 1000 °C and at a reaction time of 20 hours. This is probably due to the formation of a compact layer containing the unreacted oxides of Si, Al, or other oxides that decreases the reaction rate. Figure 7 shows that, between 850 °C and 1000 °C, the apparent activation energies E_a of the chlorination of the LGC and HGC were equal to 166 and 293 kJ/mole, respectively.

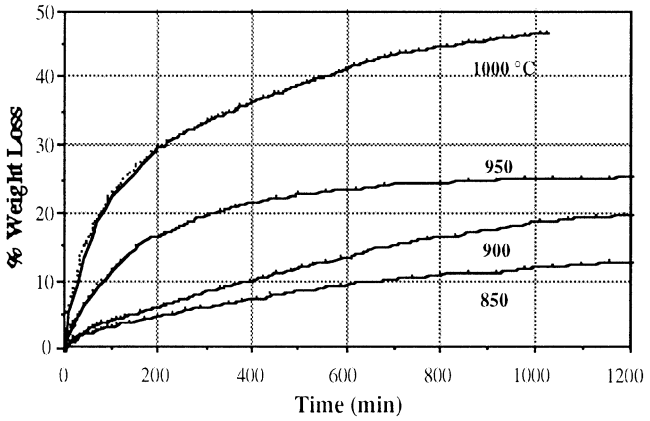

Fig. 6—Isotherms of the HGC chlorination using a chlorinating gas mixture having a Cl_2/N_2 ratio equal to one and a flow rate of 20 L/h.

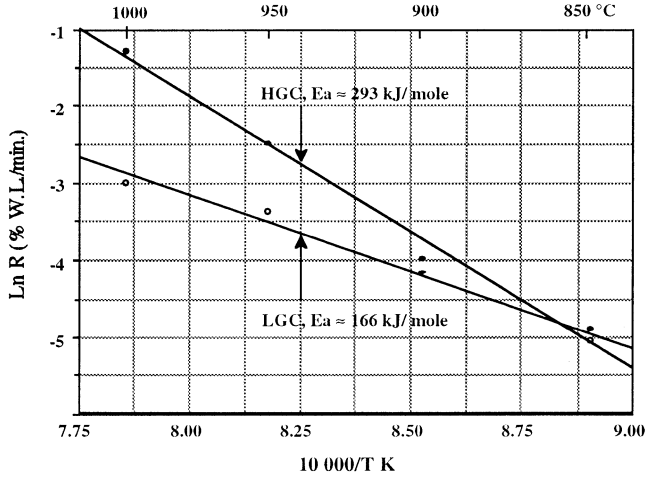

Fig. 7—Arrhenius plots of the LGC and HGC chlorination.

The values of E_a are considered approximate, because the chlorination of these two concentrates involves several reactions due to their relatively complex composition. It seems difficult to attribute a physical signification of E_a for the definition of the chlorination mechanism of these concentrates. However, the parabolic curves of Figures 5 and 6 and the high value of E_a suggest that the reaction mechanism is probably controlled by solid-state diffusion. The formation of volatile (Nb, Ta) O_2Cl or (Nb, Ta) OCl_3 will lead to a cationic deficiency on the surface of the tantalum or niobium oxides. It seems that the diffusion of the Ta and Nb ions throughout the layer of unreacted oxides and produced nonvolatile chlorides is the rate-controlling step.

For these reasons, the experimental data were processed using the mathematical correlation suggested by Szekely *et al.*[22] According to their analysis, the following equations describe reactions controlled by the diffusion for a sphere, long cylinder, and slabs, respectively.

$$kt = 1 - 3(1 - X)^{2/3} + 2(1 - X) \quad (\text{for } F_p = 3) \quad [25]$$

$$kt = X + (1 - X)\ln(1 - X) \quad (\text{for } F_p = 2) \quad [26]$$

$$kt = X^2 \quad (\text{for } F_p = 1) \quad [27]$$

where

t = chlorination time;

k = constant;

X = extent of reaction (ratio of weight of the reacted fraction to initial weight); and

F_p = particle shape factor (1 for infinite slabs, 2 for long cylinders, and 3 for spheres).

The mathematical fitting of the chlorination data was performed using Eqs. [25], [26], and [27]. However, it is difficult to confirm these models because the difference between the correlation coefficients was within the experimental errors. For the three equations, the average correlation coefficients were 0.988 and 0.998 for LGC and HGC, respectively. The formation of volatile oxychlorides, according to Figure 1, will lead to the concentration of impurities as oxide or chloride on the solid surface, thus constituting a compact layer. In these conditions, the chlorination reaction rates of LGC and HGC were controlled by the diffusion of refractory metal cations through a layer of solid and/or liquid chlorides such as $MnCl_2$ or $CaCl_2$. Such a layer constitutes a diffusion barrier. However, the low impurity level of HGC (Table I) and its dendritic shape (Figure 8) will attenuate the diffusion phenomena. This probably explains the difference between E_a for the LGC and HGC.

2. *LGC and HGC chlorination using the horizontal reactor*

In addition to the previously described TG tests, the chlorination of LGC and HGC was carried out using a $Cl_2 + N_2$ gas mixture under isothermal conditions between 350 °C and 1000 °C for a period of 24 hours using the method described in Figure 3. The use of about 5 g/test generates sufficient quantities of condensates and residues that can be examined by XRD, SEM, and chemical analysis. The amount of Nb_2O_5 and Ta_2O_5 reacted with the $Cl_2 + N_2$ gas mixture for LGC and HGC is given in Figures 9(a) and (b) as a function of temperature.

Figure 9(a) shows a decrease of the Nb_2O_5 and Ta_2O_5 chlorination extent of the LGC between 600 °C and 900 °C. This was due to the formation of a layer composed mainly of solid or liquid $MnCl_2$ or $CaCl_2$ that constituted a diffusion barrier. This decreased the mass transfer between the chlorinating gas mixture and this concentrate. The presence of $MnCl_2$ and $CaCl_2$ on the surface of the chlorination residue obtained at 700 °C was observed by SEM. The volatilization of these chlorides above 900 °C allowed higher extraction rates of tantalum and niobium compounds. Chemical analysis of the chlorinated residues indicates that almost complete chlorination of Nb_2O_5 and Ta_2O_5 was achieved at 1000 °C (Figure 9(a), Table II). However, as shown in Table III, the obtained condensates contain tantalum and niobium chlorinated compounds contaminated with iron and manganese chlorides. One may note that, in this case, the chlorination extent of Ta_2O_5 was higher than that of Nb_2O_5.

The XRD analysis revealed that, while the condensates were amorphous, the chlorination residues were crystalline. Table IV groups the identified phases detected in the reaction residues as a function of temperature. The main crystallized compounds were SiO_2, calcium niobate, and calcium tantalate. The presence of these two phases explains the relatively slow chlorination rate of the LGC compared to that of the HGC (Figures 5 and 6). This could be attributed to the formation of a $CaCl_2$ solid or liquid layer. De Freitas and Ajersch,[23] in their study of the carbochlor-

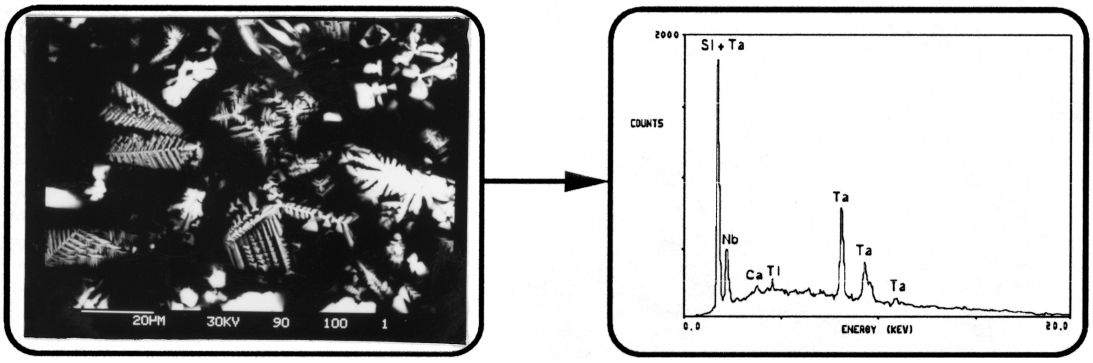

Fig. 8—Morphological aspects of HGC.

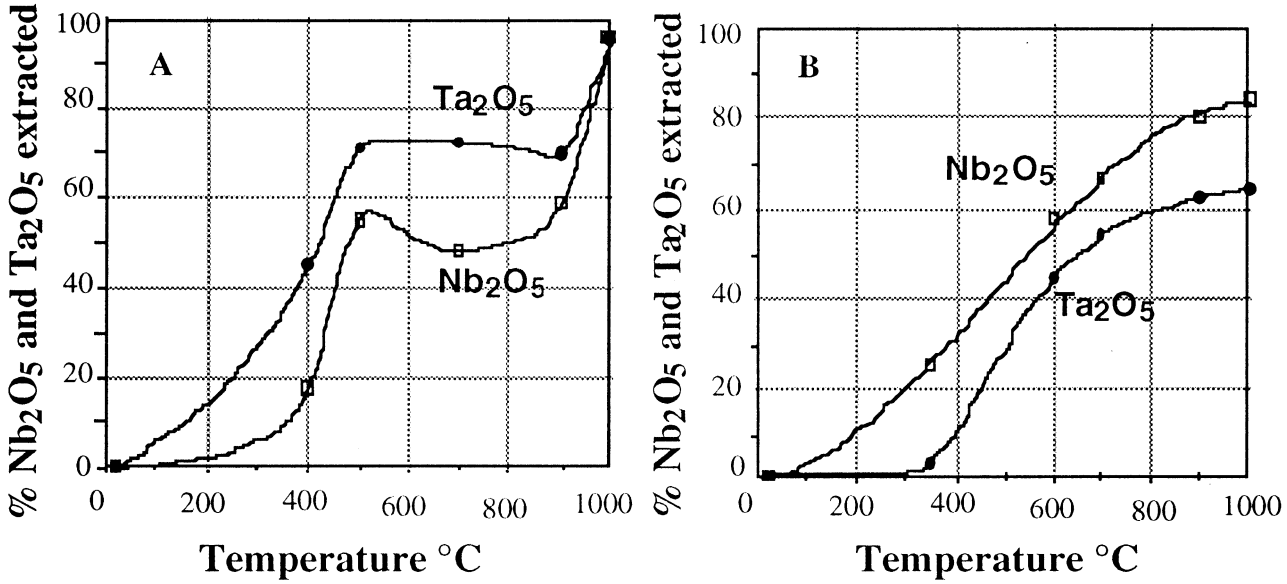

Fig. 9—Evolution of the percent of Ta_2O_5 and Nb_2O_5 extracted by the chlorination of (*a*) the LGC and (*b*) the HGC, as a function of temperature with Cl_2/N_2 molar ratio equal to 1.

Table II. Chemical Composition of the LGC Chlorination Residues (Weight Percent)

	Initial	400 °C	500 °C	900 °C	1000 °C
Pct weight loss	—	17.7	24.7	27.8	47.3
Pct Ta_2O_5	13.7	9.2	5.3	5.8	1.2
Pct E. Ta_2O_5*	—	44.9	71.1	69.7	95.6
Pct Nb_2O_5	6.3	6.3	3.7	3.6	0.5
Pct E. Nb_2O_5	—	17.7	55.5	59.0	96.0
Ta_2O_5/Nb_2O_5	2.2	1.5	1.4	1.6	2.4

*Pct E. = percent extracted of a specific oxide.
Pct E. = 100 − ((pct metal oxide content in residue ∗ (100 − pct weight loss))/pct initial metal oxide content).

Table III. Qualitative Composition of the LGC Chlorination Products Obtained by SEM

T (°C)	Residues*	Condensates
Initial	Ca, Si, Ta, Mn, Nb, Ti, Fe, Al	—
400	Ca, Si, Mn, Ta, Nb, Fe, Ti, Al	Ta, Cl, Nb, ε** Fe
500	Ca, Si, Mn, Ta, Nb, Ti, Fe, Al	Ta, Fe, Cl, Nb
700	Ca, Si, Ta, Mn, Nb, Fe, Ti, Al	Ta, Cl, Fe, Nb, ε Mn
900	Ca, Si, Ta, Mn, Ti, Nb, Al	Cl, Mn, Nb, Fe, Ta
1000	Ca, Si, Ta, Ti, Al	Cl, Ta, Mn, Nb, Fe

*Residues dechlorinated at 1000 °C.
**ε: traces.

ination of calcium niobate, confirmed this assumption. They observed the formation of a $CaCl_2$ solid layer following Eq. [28]. In the present case, the formation of a solid and/or liquid layer of $CaCl_2$ and $MnCl_2$ will decrease the chlorination rate of the LGC.

$$CaNb_2O_6\ (s) + 4\ Cl_2\ (g) + 4CO\ (g) \rightarrow CaCl_2\ (s) + 2\ NbOCl_3\ (g) + 4\ CO_2\ (g) \quad [28]$$

Figure 9(b) shows the extraction rate of Ta and Nb oxides determined by chemical analysis during the chlorination of HGC between 350 °C and 1000 °C. This figure indicates that the extraction percent of Nb_2O_5 and Ta_2O_5 increased continuously as a function of temperature. This is due to the lower content of impurities in the HGC. However, it should be noted that the total amount of Nb_2O_5 and Ta_2O_5 reacted (Table V) during the HGC chlorination was lower than that obtained for the LGC. This may be attributed to the formation of gaseous complex metal chlorides, such as (Nb, Ta)$FeCl_8$ and (Nb, Ta)$AlCl_8$, that could enhance the extraction of refractory metals chlorides in the LGC case.[24,25]

Table IV. Compounds Identified by XRD in the LGC Chlorination Residues

	JCPDS File	Initial*	400 °C	500 °C	700 °C	900 °C	1000 °C
SiO_2	11-695	▒	▒	▒	▒	■	■
$CaNb_2O_6$	31-289	■	■	■	■	□	□
$CaTa_2O_6$	29-385	■	■	■	■	■	▒

*Heated at 1000 °C in N_2; ■ major phase; ▒ minor phase; and □ not detected.

Table V. Chemical Composition of the HGC Chlorination Residues (Weight Percent)

	Initial	350 °C	600 °C	700 °C	900 °C	1000 °C
Pct weight loss	—	13.0	43.2	62.9	70.7	73.7
Pct Ta_2O_5	34.9	38.9	34.1	43.2	44.8	47.4
Pct E. Ta_2O_5	—	3.1	44.5	54.0	62.5	64.5
Pct Nb_2O_5	28.3	24.5	21.2	25.7	19.2	17.3
Pct E. Nb_2O_5	—	24.7	57.4	66.3	80.2	83.9
Ta_2O_5/Nb_2O_5	1.2	1.6	1.6	1.7	2.3	2.7

*Pct E. = percent extracted of a specific oxide.
Pct E. = 100 − ((pct metal oxide content in residue * (100 − pct weight loss))/pct initial metal oxide content).

Table VI. Qualitative Composition of the HGC Chlorination Products (SEM)

T (°C)	Residues*	Condensates
Initial	Ta, Si, Nb, ε** (Ti, Ca)	—
350	Ta, Si, Nb, ε (Ti, Ca)	Nb, Cl
400	Si, Ta, Nb, ε (Ti, Cl, Ca)	Nb, Ta, Cl
600	Si, Ta, Nb, ε (Cl, Ti, Ca)	Ta, Nb, Cl
700	Si, Ta, Nb, ε (Ti, Ca)	Nb, Cl, Ta
1000	Si, Ta, Nb, ε (Ti, Ca)	Nb, Cl, Ta

*Residues dechlorinated at 1000 °C.
**ε: traces.

Table V indicates that the extraction of niobium was higher than that of tantalum in the investigated temperature range. This leads to an increase of the Ta_2O_5/Nb_2O_5 weight ratio in the residue and to an enrichment of the condensates in niobium chlorides and/or oxychlorides (Table VI). This clearly indicates that chlorination of the HGC permits the recovery of purer tantalum and niobium chlorinated compounds as compared to the chlorination of the LGC.

Table VII presents the XRD analysis of identified phases contained in the HGC chlorination residues as a function of temperature. Ta_2O_5, Nb_2O_5, SiO_2, and compounds such as $Nb_2CaTa_4O_{11}$ and $FeNb_{49}O_{124}$ were detected.

The chlorination of LGC and HGC with an equimolar Cl_2-N_2 gas mixture could be considered unsatisfactory. In the first case, the tantalum and niobium extraction was almost complete, but the purity of their recovered chlorinated compounds was relatively low. In the latter case, the purity was higher, but the extraction of these refractory metals' compounds was incomplete. The best results were obtained at 1000 °C. In addition to important energy consumption, such high temperatures will increase reactor corrosion problems. For these reasons, carbochlorination of these concentrates was investigated. Results are summarized later.

B. *Carbochlorination of LGC and HGC by Cl_2 + CO + N_2*

As for the case of chlorination, the kinetics of carbochlorination of LGC and HGC was studied using nonisothermal and isothermal TG measurements. A Cl_2 + CO + N_2 (1/1/1) gas mixture with a total flow rate of 30 L/h was used.

1. *Kinetic study in nonisothermal conditions*

Figure 10 compares the carbochlorination percent weight loss of the LGC to that of the HGC as a function of temperature. Carbochlorination reactions of HGC and LGC started at about 400 °C. However, reactivity of the HGC toward the carbochlorinating gas mixture was higher than that of the LGC. As previously mentioned, the lower carbochlorination extent of the LGC was probably due to the formation of a solid and/or liquid layer of Mn or Ca chlorides that acts as a diffusion barrier. On the other hand, as expected, the carbochlorination extent of the two concentrates was higher than for the chlorination case (Figures 4 and 10).

2. *Kinetic study in isothermal conditions*

The evolution of the LGC and HGC weight loss as a function of carbochlorination reaction time at different temperatures is given in Figures 11 and 12. The related Arrhenius plots are grouped in Figure 13. The apparent activation energy of the carbochlorination of LGC changes from 116 to about 80 kJ/mole for temperatures lower than 650 °C and higher than 800 °C, respectively. The E_a of the carbochlorination of HGC was about 103, 10, and 34 kJ/mole for the temperature ranges of 350 °C to 450 °C, 450 °C to 600 °C, and 800 °C to 950 °C, respectively. The values of E_a are given as an indication of the evolution of the reaction kinetics as a function of temperature.

The Arrhenius plot for the carbochlorination of LGC and HGC exhibits an anomaly in the temperature range of about 600 °C to 800 °C (Figure 13). Similar anomalies were observed during the carbochlorination of several metal oxides within approximately the same temperature range[18,26,27,28] (Figure 14). The authors attributed this phenomenon to full decomposition of $COCl_2$ at temperatures higher than 600 °C according to Eq. [29]. One should emphasize that this gas was formed *in situ* when using Cl_2 + CO gas mixtures. However, the Arrhenius plot anomaly observed for the carbochlorination of LGC could also be attributed to the formation of a liquid layer of $MnCl_2$ (melting point = 650 °C).

$$COCl_2 \rightarrow Cl_2 + CO \qquad [29]$$

A comparison between Figures 13 and 14 shows that the reaction rate of the LGC is systematically lower than that

Table VII. Compounds Identified by XRD in the HGC Chlorination Residues

Compounds	JCPDS File	Initial*	350 °C	600 °C	700 °C	1000 °C
Ta_2O_5	25-922	■	■	■	■	■
$CaTa_4O_{11}$	15-679	□	▒	▒	▒	▒
Nb_2O_5	27-1003	■	■	■	■	■
$FeNb_{49}O_{124}$	22–351	■	■	□	□	□
SiO_2	11-695	▒	▒	▒	■	■

*Heated at 1000 °C in N_2; ■ major phase; ▒ minor phase; and □ not detected.

of pure compounds. This is attributed to the presence of a high impurity content. The HGC has a reaction rate comparable to that of pure compounds.

As mentioned in Section V–A–1, the values of E_a are approximate, because the chlorination of these two concentrates involves several reactions due to their relatively complex composition. In these conditions, determination of the reaction mechanism is difficult. However, as suggested by Szekely *et al.*,[22] the evolution of E_a (Figure 13) could be interpreted by the change of the control of the reaction mechanism from chemical kinetics at low temperatures to diffusion or mass transfer control at high temperatures. The comparison between the forms of the curves obtained at low and high reaction temperatures (Figures 11 and 12) agrees with this hypothesis.

3. *Carbochlorination of the LGC and HGC using the horizontal reactor*

A series of experiments was performed using 5 g of the LGC or HGC per test to study the evolution of the carbochlorination products by XRD, SEM, and chemical analysis. These trials were carried out between 200 °C and 1000 °C, for 24-hour runs using a Cl_2-CO-N_2 (1/1/1) gas mixture having a total flow rate of 30 L/h.

a. *Carbochlorination of the LGC*

Figure 15 displays the amount of tantalum and niobium oxides reacted determined by the chemical analysis of the residues of carbochlorination as a function of temperature. The extraction rate of tantalum and niobium compounds decreases between about 600 °C and 800 °C. Comparing Figure 15 to Figure 9(a) indicates the extraction of tantalum and niobium compounds is almost equivalent and independent of the chlorinating gas mixture. As explained previously, the combined effects of the formation of a liquid layer of $MnCl_2$ and that of $COCl_2$ dissociation are probably responsible for this phenomenon.

Table VIII gives the weight loss obtained during the LGC carbochlorination by the $Cl_2 + CO + N_2$ mixture, the weight percent of Ta_2O_5 and Nb_2O_5 remaining in the residues, and the percent of their reaction as determined by the chemical analysis of the carbochlorination residues. The weight loss of the LGC carbochlorination was almost 20 pct higher than that of its chlorination (Table II). This is due to the partial carbochlorination of oxides such as Al_2O_3, TiO_2, and SiO_2 that were not chlorinated in the absence of carbon monoxide. During the carbochlorination, the extraction of tantalum compounds was systematically higher than that of the niobium compounds, leading to a decrease of the Ta_2O_5/Nb_2O_5 ratio in the residue as the temperature increased.

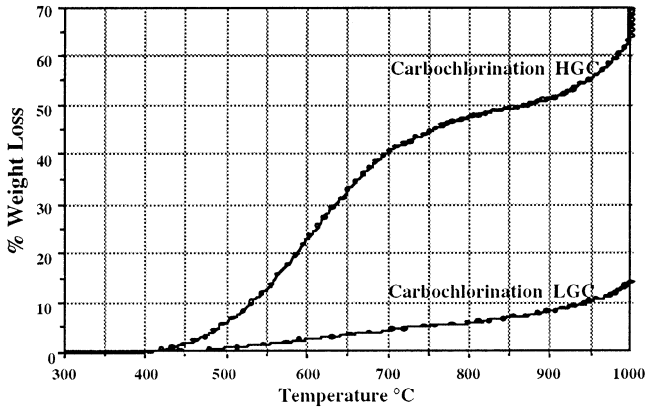

Fig. 10—Carbochlorination of the LGC and HGC under nonisothermal conditions (heating rate = 25 °C/min).

The residues and condensates of the LGC carbochlorination were analyzed by SEM. Results are given in Table IX. As expected, elements such as calcium and silicon were concentrated in the residues, while Ta, Nb, Fe, Mn, Al, and Ti chlorinated compounds were volatilized and recovered in the condensate. The tantalum and niobium-bearing condensates were contaminated with iron and manganese chlorides as was the case for the chlorination (Table III).

Table X presents the XRD analysis of the phases detected in the carbochlorination residues as a function of temperature. The main crystallized compounds were SiO_2, calcium tantalate, and calcium niobate. The carbochlorination rate of these compounds is relatively smaller than that of simple tantalum and niobium pentoxides. This may explain the relatively slow carbochlorination kinetics of the LGC compared to those of HGC.

b. *Carbochlorination of the HGC*

Table XI shows the experimental data of the carbochlorination of the HGC. It includes the percent weight loss of the samples during its carbochlorination between 200 °C and 500 °C. It also indicates the weight percent of Ta_2O_5 and Nb_2O_5, obtained by chemical analysis, in the carbochlorination residue and the Ta_2O_5/Nb_2O_5 ratio. This ratio increases in the residues of the carbochlorination as a function of temperature up to 300 °C.

Figure 16 shows the amount of extracted tantalum and niobium compounds as a function of temperature. This figure indicates that the carbochlorination of Nb_2O_5 was complete at about 300 °C and that of Ta_2O_5 at 500 °C. The presence of small amounts of Ca, Fe, and Mn compounds in the HGC and the use of reducing agent in the chlorinating gas mixture allows complete extraction of tantalum and

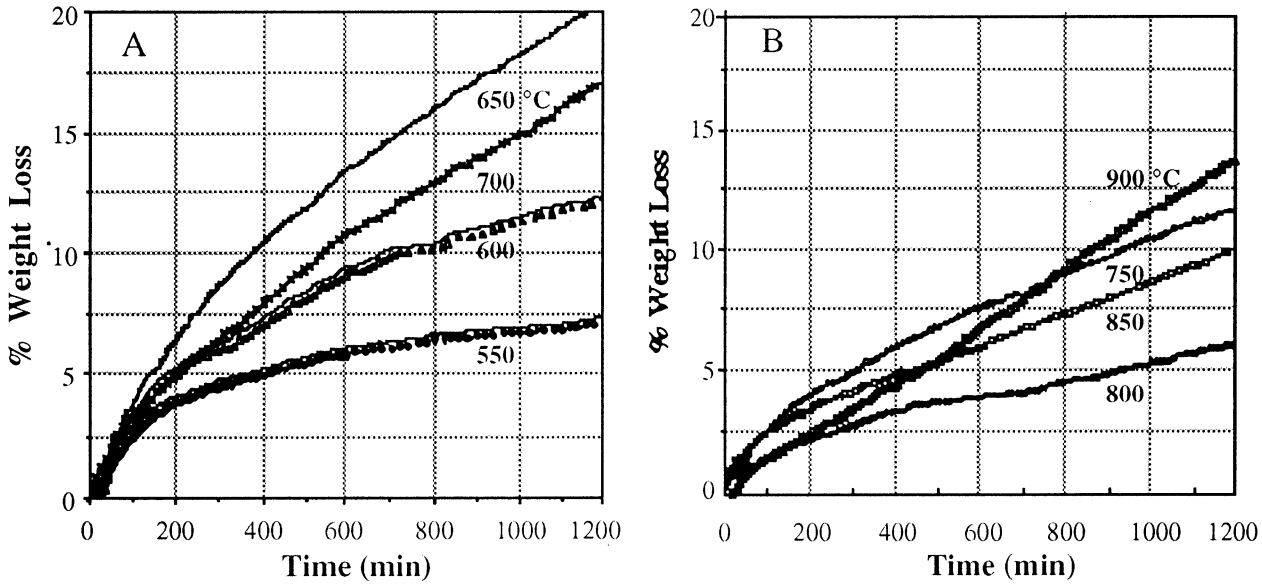

Fig. 11—Isotherms of the LGC carbochlorination at (*a*) T ≤ 700 °C and (*b*) *T* ≥ 750 °C.

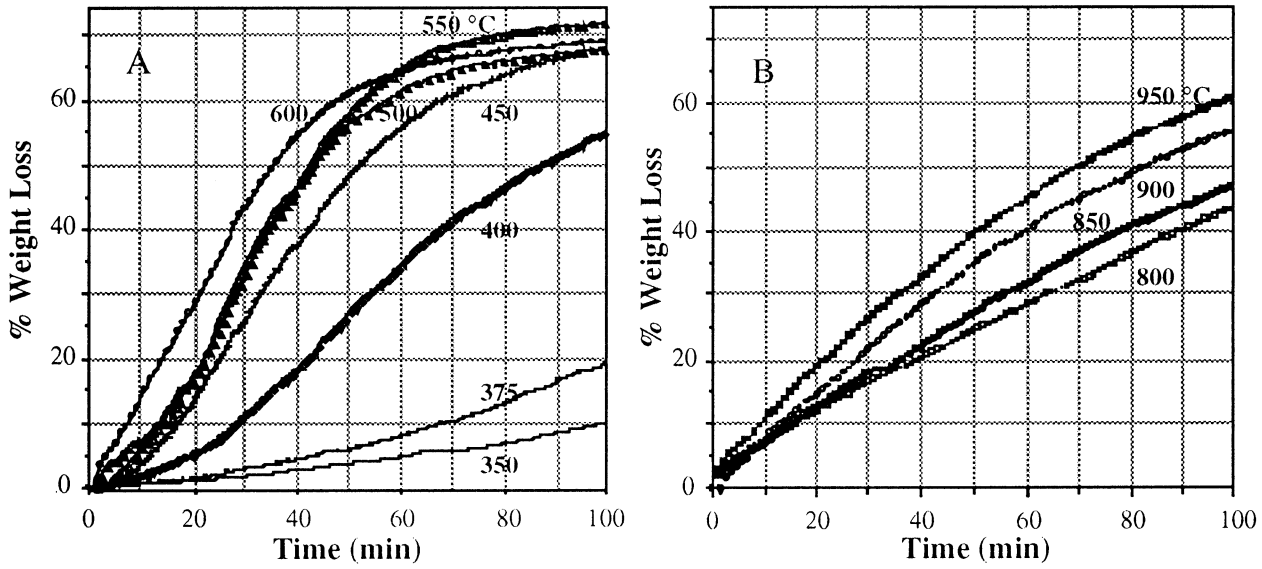

Fig. 12—Isotherms of the HGC carbochlorination at (*a*) *T* ≤ 600 °C and (*b*) *T* ≥ 800 °C.

niobium compounds from their concentrate at relatively low temperatures (<500 °C). Figures 16 and 9(b) show that the carbochlorination of HGC is more efficient than its chlorination.

The evolution of the qualitative composition of residues and condensates obtained by the carbochlorination of the HGC as a function of temperature is given in Table XII. The condensates were essentially composed of tantalum and niobium chlorinated compounds. Purification of such condensates should be easier than those obtained by the carbochlorination of the LGC (Table IX).

Table XIII presents the different phases detected by XRD in the carbochlorination residues as a function of temperature. These residues were mainly composed of silicon, tantalum, and niobium oxides. Small amounts of $CaTa_4O_{11}$ and $FeNb_{49}O_{124}$ were also identified. It should be noted that $CaTa_4O_{11}$ was not chlorinated at 300 °C. This compound is more difficult to chlorinate than tantalum pentoxide.

Results of Figures 9(a) and 15 indicate that chlorinating or carbochlorinating LGC gives almost the same extraction rate of the tantalum and niobium compounds. However, carbochlorination of the HGC leads to much better results than chlorination (Figures 9(b) and 16). It confirms the benefits of previous efficient leaching of tin slag before subsequent halogenation.

VI. CONCLUSIONS

Extraction of tantalum and niobium compounds was studied by chlorination and carbochlorination of two concentrates obtained by the leaching of tin slag. They were designated as LGC and HGC, and they contain 23 and 59 pct of $Ta_2O_5 + Nb_2O_5$, respectively.

The reactivity of HGC, with respect to a $Cl_2 + N_2$ gas mixture, is higher than that of LGC. In nonisothermal conditions, the chlorination of these two concentrates starts at

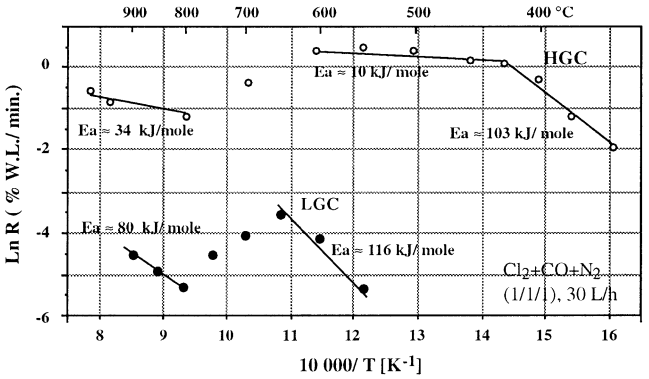

Fig. 13—Arrhenius plots for the carbochlorination of LGC and HGC.

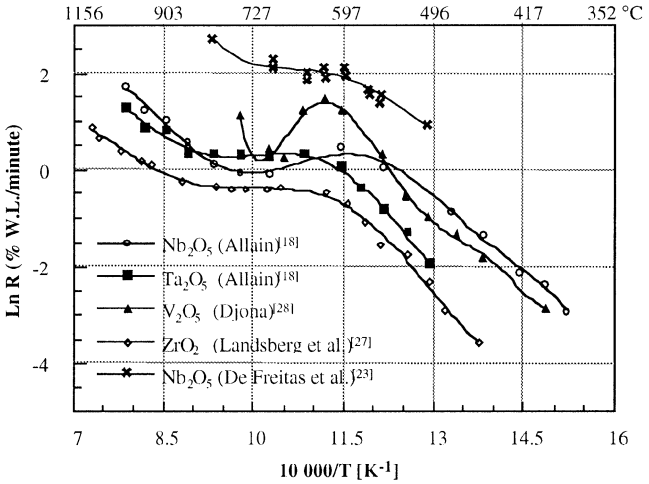

Fig. 14—Comparison of Arrhenius plots of the carbochlorination of various metal oxides.

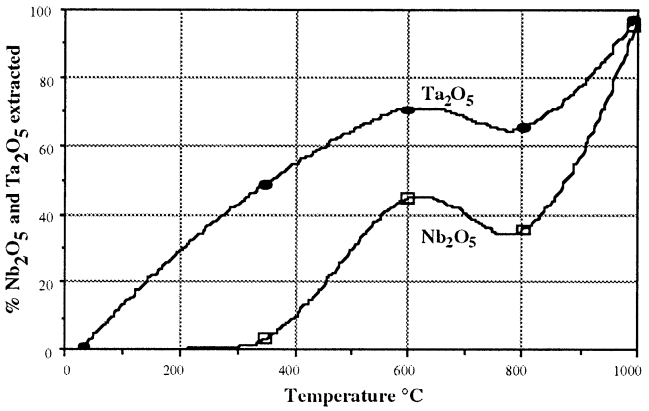

Fig. 15—Evolution of the percent of Ta_2O_5 and Nb_2O_5 extracted by carbochlorination of the low-grade concentrate, as a function of temperature (reaction time = 24 h).

about 400 °C and leads to the formation of volatile chlorinated metal compounds. The condensates of the chlorination of HGC are purer than those of the LGC. During chlorination, the unreacted compounds, such as SiO_2, Al_2O_3, and chlorides of Ca and Mn, constitute a layer that decreases the mass transfer between the concentrate particles and the chlorinating gas mixture leading to a decrease of reaction rate. The apparent activation energies E_a for the chlorination of HGC and LGC between 850 °C and 1000 °C were 293 and 166 kJ/mole, respectively. The chlorination rate seemed to be limited by the solid-state diffusion of refractory metal ions through the formed layer. One may underline that the thickness of such a layer is smaller for HGC than that for LGC due to the lower level of impurities in HGC.

Table VIII. Chemical Composition of the LGC Carbochlorination Residues (Weight Percent)

	Initial	350 °C	600 °C	800 °C	1000 °C
Pct weight loss	—	16.9	44.8	38.0	69.6
Pct Ta_2O_5	13.7	8.4	7.2	7.6	0.3
Pct E. Ta_2O_5*	—	52.0	70.9	65.4	99.4
Pct Nb_2O_5	6.3	7.3	6.3	6.6	0.3
Pct E. Nb_2O_5	—	9.4	44.8	35.2	98.4
Ta_2O_5/Nb_2O_5	2.2	1.1	1.1	1.2	0.8

*Pct E. = percent extracted of a specific oxide.
Pct E. = 100 − ((pct metal oxide content in residue ∗ (100 − pct weight loss))/pct initial metal oxide content).

Table IX. Qualitative Composition of the LGC Carbochlorination Products (SEM)

T (°C)	Residues*	Condensates
Initial	Ca, Si, Ta, Mn, Nb, Ti, Fe, Al	—
300	Ca, Si, Ta, Mn, Nb, Ti, Fe, Al	Ta, Nb, Cl, ε** Fe
400	Ca, Si, Mn, Ta, Nb, Fe, Ti, Al	Ta, Nb, Cl, ε Fe
600	Ca, Si, Mn, Ta, Nb, Fe, Ti, ε Al	Cl, Ta, Fe, Nb
800	Ca, Si, Ta, Nb, Mn, Ti, ε (Fe, Al)	Cl, Ta, Nb, Fe, Ti, Mn
1000	Ca, Si	Cl, Ta, Nb, Fe, Mn, ε Ti

*Residues dechlorinated at 1000 °C.
**ε: traces.

More than 95 pct of tantalum and niobium compounds were extracted by the chlorination of the LGC at 1000 °C for 24 hours. Between 600 °C and 900 °C, the chlorination rate of the LGC remained almost constant due to the formation of a layer composed of solid and/or liquid Ca and Mn chlorides containing the unreacted oxides of Si and Al. The obtained condensates were composed of tantalum and niobium chlorinated compounds contaminated by the iron and manganese chlorides. For the same experimental conditions, only 65 pct of tantalum and 84 pct of niobium compounds were recovered during the chlorination of HGC. The obtained condensates were composed of almost pure tantalum and niobium chlorinated compounds. The recovery rates of tantalum and niobium compounds by the chlorination of LGC were higher than those of HGC probably due to the synthesis of gaseous complex metal chlorides (GCMC) such as (Nb, Ta)$FeCl_8$ and (Nb, Ta)$AlCl_8$. These GCMCs increase the vapor pressure of simple refractory metal chlorides.

Use of TGA revealed that the reactivity of HGC toward the carbochlorinating gas mixture $Cl_2 + CO + N_2$ was higher than that obtained by the chlorinating gas mixture. For LGC, no appreciable difference was observed. Carbochlorination of these concentrates started at about 400 °C.

The Arrhenius plot for the carbochlorination of LGC and HGC exhibits an anomaly between 600 °C and 800 °C that

Table X. Compounds Identified by XRD in the LGC Carbochlorination Residues

	JCPDS File	Initial*	350 °C	500 °C	600 °C	800 °C	1000 °C
SiO_2	11-695	▒	▒	▒	▒	■	■
$CaSiO_3$	27-1064	□	□	□	□	□	■
$CaNb_2O_6$	31-289	■	■	■	■	■	□
$CaTa_2O_6$	29-385	■	■	■	■	■	□

*Heated at 1000 °C in N_2; ■ major phase; ▒ minor phase; and □ not detected.

Table XI. Chemical Composition of the HGC Carbochlorination Residues (Weight Percent)

	Initial	200 °C	225 °C	250 °C	300 °C	500 °C
Pct weight loss	—	40.4	61.4	68.5	79.9	92.0
Pct Ta_2O_5	28.0	33.9	32.9	35.1	22.8	5.7
Pct E. Ta_2O_5*	—	27.9	54.8	60.5	83.7	98.4
Pct Nb_2O_5	31.8	16.5	13.0	4.6	2.0	1.1
Pct E. Nb_2O_5	—	69.1	84.2	95.5	98.7	99.7
Ta_2O_5/Nb_2O_5	0.9	2.1	2.5	7.7	11.4	5.1

*Pct E. = percent extracted of a specific oxide.
Pct E. = 100 − ((pct metal oxide content in residue ∗ (100 − pct weight loss))/pct initial metal oxide content).

Table XII. Qualitative Composition of the HGC Carbochlorination Products (SEM)

T (°C)	Residues*	Condensates
Initial	Ta, Si, Nb, ε** Ca	—
200	Ta, Si, Nb, Ca, ε (Ti, Mn, Fe)	Ta, Nb, Cl
250	Si, Ta, Ca, Nb, ε Ti	Ta, Nb, Cl
300	Si, Ta, Ca, ε (Nb, Mn, Fe)	Ta, Nb, Cl, ε Ti
500	Ca, Si, Ta, ε (Cl, Mn, Fe)	Ta, Cl, Nb
700	Si, Ca, Ta	Ta, Cl, Nb

*Residues dechlorinated at 1000 °C.
**ε: traces.

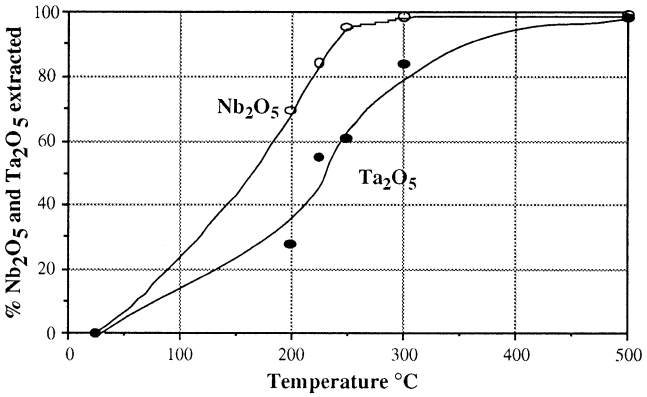

Fig. 16—Percent of Ta_2O_5 and Nb_2O_5 reacted as a function of temperature during the carbochlorination of the HGC.

can be attributed to complete decomposition of $COCl_2$ formed *in situ*. The formation of a layer of solid and/or liquid chlorides of Mn and Ca may also contribute to this rate anomaly in the case of the LGC. The apparent activation energies of the carbochlorination of the LGC and the HGC were 116 and 103 kJ/mole for temperatures lower than 650 °C and 450 °C, respectively.

More than 95 pct of tantalum and niobium compounds were extracted by the carbochlorination of the LGC at 1000 °C for a reaction time of 24 hours. The obtained condensates were contaminated by Fe, Ca, and Mn chlorides. Full extraction of tantalum and niobium compounds contained in the HGC was possible at temperatures ≤500 °C for a reaction time of 24 hours. Furthermore, the compounds of niobium and tantalum obtained in the condensates were almost pure.

These results show the advantages of a previous leaching of tin slag in order to obtain a high-grade concentrate before its subsequent chlorination. On the other hand, the carbochlorination of the high-grade concentrate, at relatively low temperatures, could be an efficient process for the extraction of pure tantalum and niobium compounds from the tin slag.

ACKNOWLEDGMENTS

Part of this work was carried out within the framework of Convention No. 500 of Plan Métaux, Fédération des Chambres Syndicales des Minerais et Métaux Bruts. Thanks to M. Houze, Département de l'Energie et des Ma-

Table XIII. Phases Identified by XRD in the HGC Carbochlorination Residues

Compounds	JCPDS File	Initial*	200 °C	225 °C	250 °C	300 °C	500 °C
Ta_2O_5	25-922	■	■	■	■	▒	□
Nb_2O_5	27-1003	■	■	■	■	▒	□
$CaTa_4O_{11}$	15-679	□	▒	■	■	■	□
$FeNb_{49}O_{124}$	22-351	■	□	□	□	□	□
SiO_2	11-695	▒	▒	▒	▒	■	■

*Heated at 1000 °C in N_2; ■ major phase; ▒ minor phase; and □ not detected.

tières Premières, French ministry of the industry. This research was also partially funded by the European Union in the framework of Research Contract No. MA1M-0071-C(CD). The authors thank Dr. M. Donato (EU, DG-XII) for help and discussions.

The authors would like to thank Drs. R. Solozabal and J.C. Mugica (INASMET, San Sebastian, Spain) for providing samples and technical discussions. The authors are also indebted to Messrs. A. Bonazebi, S. Ivanaj, N. Kanari, N. Menad, and N. Mirghaffari for discussions and help on different subjects and to Mrs. V. Ivanaj for technical and administrative support.

REFERENCES

1. R.J. Tolley: Tantalum-Niobium International Study Center, 40 rue Washington, 1050 Brussels, Belgium, 1992, No. 69, p. 3.
2. R. Stienning: *Proc. Int. Symp. on Tantalum and Niobium*, Orlando, Florida, USA, published by T.I.C., 40 rue Washington, 1050 Brussels, Belgium, 1988, pp. 725-45.
3. L.C. Cunningham: *Mineral Commodity Summaries*, United States Department of the Interior, Bureau of Mines, Washington, DC, 1991, pp. 44-45.
4. F.W. Clarke: *Bull. Phil. Soc.*, 1889, vol. 11, p. 131.
5. Anonymous: L'usine Nouvelle, 1996, No. 2545, p. 109.
6. A. Murciego: Ph.D. Thesis, University of Salamanca, Salamanca, Spain, 1990.
7. G.L. Miller: *Metallurgy of the Rarer Metals*, H.M. Finniston, ed., LBS, London, 1959, pp. 71-75.
8. W.W. Albrecht and W. Rockenbauer: *Proc. Int. Conf. on Tantalum and Niobium*, Orlando, Florida, USA, published by T.I.C., 40 rue Washington, 1050 Brussels, Belgium, 1988, pp. 219-40.
9. W.W. Albrecht, W. Bludssus, J. Eckert, W. Rockenbauer, and H.C. Stark: *Tantalum-Niobium International Study Center*, 40 rue Washington, 1050 Brussels, Belgium, 1990, No. 64, pp. 5-9.
10. I. Gaballah and E. Allain: *Metall. Trans. B*, 1992, vol. 23B, pp. 249-59.
11. F.E. Block: Paper presented at Int. Conf., Achema, Frankfurt, Germany, 1958.
12. D.H. Lee: *J. Kor. Inst. Mineral Mining Eng.*, 1982, vol. 19, pp. 209-14.
13. S.L. May and G.T. Engel: U.S. Bureau of Mines, Cochrans Mill Road, P.O. Box 18070, Pittsburgh, PA, 15236-0070, 1958, R.I. No. 6635.
14. F.J. Moura, E. de A. Brocchi, and H.M. Kolher: *Pyrometallurgy 87 Symp.*, N. Warner, ed., IMM, London, 1987, pp. 799-812.
15. E. de A. Brocchi: Ph.D. Thesis, Imperial College of Science and Technology, University of London, London, 1983.
16. E. de A. Brocchi and J.H.E. Jeffes: *Conf. of Mineral Processing Metallurgy*, M.J. Jones and P. Gill, eds., IMM, London, 1984, pp. 161-70.
17. E. Allain, I. Gaballah, and M.-Ch. Meyer: Final Report of ''Convention 500 du Plan Métaux,'' INPL, Nancy, France, 1987.
18. E. Allain: Ph.D. Thesis, University of Nancy I, Nancy, France, 1993.
19. A. Roine: *Outokumpu HSC Chemistry for Windows*, version 2.0, Outokumpu Research, Pori, Finland, May 1994.
20. I. Gaballah, E. Allain, and M.C. Meyer: *Proc. Int. Symp. on Refractory Metals*, K. Nona, C. Lidell, D.R. Sadoway, and R.G. Bautista, eds., TMS, New Orleans, LA, 1990, pp. 283-96.
21. I. Gaballah, E. Allain, M.C. Meyer, and K. Malau: *Metall. Mater. Trans. B*, 1994, vol. 25B, pp. 193-205.
22. J. Szekely, J.W. Evans, and H.Y. Sohn: *Gas-Solid Reactions*, Academic Press, New York, NY, 1976, pp. 68-70, 73-88, 109-31, and 232-35.
23. L.R. De Freitas and F. Ajersch: *Can. Metall. J.*, 1986, vol. 25 (3), pp. 219-24.
24. H.A. Øye and D.M. Gruen: *J. Am. Chem. Soc.*, 1969, vol. 91 (9), pp. 2229-36.
25. I. Gaballah and N. Kanari: *Proc. 7th Nat. Conf. on Metallurgical Science and Technology*, Madrid, Spain, 1990, pp. 377-86.
26. M.K. Soleiman and I.K. Rao: *Metall. Trans. B*, 1987, vol. 18B, pp. 459-70.
27. A. Landsberg, C.L. Hoatson, and F.E. Block: *Metall. Trans. B*, 1972, vol. 3B, pp. 517-23.
28. I. Gaballah, M. Djona, and E. Allain: *Metall. Mater. Trans. B*, 1995, vol. 26B, pp. 711-18.